SPECTRAL AEROSOL OPTICAL THICKNESS RETRIEVAL USING POLARIZATION MEASUREMENTS FROM SPACE

Kazuhiko Masuda*, Masayuki Sasaki, Hiroshi Ishimoto, and Tsutomu Takashima
Meteorological Research Institute, Tsukuba, Ibaraki, 305-0052 Japan

1.INTRODUCTION

Atmospheric aerosols play an important role in the Earth radiation budget directly by scattering and absorbing solar and terrestrial radiation and indirectly by changing cloud properties. Accurate evaluation of their effects on the climate requires global information on aerosol properties. Such global information can only be acquired using satellite remote sensing. It is advantageous to use the polarization information for retrieving the aerosol optical properties because the degree of polarization can be determined without making absolute measurements and it involves only relative intensity components of the Stokes vector.

Masuda et al. (1999) investigated the feasibility of using polarization measurements from ships to retrieve aerosol optical properties over the ocean. They retrieved aerosol optical thickness at λ=550nm ($\tau_{a,550}$) and the Ångström exponent, which is the index α when the relationship between the wavelength (λ) (μm) and the aerosol optical thickness ($\tau_{a,\lambda}$) is expressed by $\tau_{a,\lambda}=\beta\lambda^{-\alpha}$ (Ångström,1964), from polarization measurements at λ= 443nm and 865nm by referring to a look-up table.

The Polarization and Directionality of the Earth's Reflectances (POLDER) instrument (Deschamps, 1994) on board the Advanced Earth Observing Satellite (ADEOS) measured the degree and direction of polarization as well as the intensity of radiation from November 1996 to June 1997. Masuda et al. (2000b) applied the algorithm proposed by Masuda et al. (1999) to the polarization measurements by ADEOS/POLDER. In this paper, we describe a method to retrieve $\tau_{a,550}$ and α using the radiance and degree of polarization measurements from space.

* Corresponding author address: Kazuhiko Masuda, Meteorological Research Institute, Tsukuba, Ibaraki, 305-0052 Japan, e-mail: masuda@mri-jma.go.jp

2.POLDER ON BOARD ADEOS SATELLITE

POLDER consists of wide-field-of-view tele-centric optics, a rotating wheel with spectral and polarizing filters, and a two-dimensional CCD detector array (Deschamps, 1994). The polarization measurements are done at three wavelengths, 443, 670, and 865nm. Three elements of the Stokes parameter, I, Q, and U are obtained. The degree of polarization is obtained by $p(\%)=100 \times (Q^2+U^2)^{1/2}/I$. The CCD array is composed of 242 × 274 independent sensitive areas. The directional measurements cover up to 43° in the along-track direction and up to 51° in the cross-track direction. The ground pixel size is about 6km×7km at nadir. Multiple angle viewing is achieved by overriding successive images of the same spectral band. Thus, in a single satellite pass, any target within the instrument swath can be observed quasi-simultaneously from up to 14 different viewing angles. The data used in this study is a LEVEL 1 product acquired on April 26, 1997 over the ocean around Japan.

3.ATMOSPHERE-OCEAN SYSTEM MODEL

Upward radiation at the top of the atmosphere was computed by the doubling-adding method for wavelengths (λ) of 670nm and 865nm. A plane-parallel and vertically inhomogeneous atmosphere is simulated by four homogeneous sublayers (0 to 2km, 2 to 5km, 5 to 13km, and 13 to 100km). The optical thicknesses of molecular scattering and absorbent constituents were obtained from LOWTRAN7 for the midlatitude summer model (Kneizys et al, 1988). The depolarization factor of atmospheric molecules is 0.0295 according to Kneizys *et al.* (1980).

According to Radiation Commission reports (WCP-55, 1983, WCP-112, 1986), basic components of the maritime aerosol model are generally the "oceanic (OC)" model for the particles generated at the sea surface and the "water soluble (WS)" model for aerosols soluble in water and consisting of a mixture of sulfate, nitrate, and organic components. In this study, an

externally mixed model of these aerosol components is assumed. The size distribution for each aerosol model is expressed by the log-normal function. The median radius (r_m) and σ in the log function are 0.3μm and 2.51 for the OC model (WCP-112, 1986), and 0.0285μm and 2.015 for the WS model (WCP-55, 1983). Note that the σ value of the WS model has been decreased by 10% from the original value of 2.239 reported by WCP-55. The refractive indices at λ=670nm and 865nm are $1.38\text{-}i3.22\times10^{-8}$ and $1.37\text{-}i1.20\times10^{-6}$ for the OC model, and $1.53\text{-}i6.59\times10^{-3}$ and $1.52\text{-}i1.21\times10^{-2}$ for the WS model. The scattering matrices are computed by the Mie scattering theory for radii ranging from 0.001μm to 10.0μm assuming the shape of aerosol particles to be spherical. We define f_w as a ratio of the optical thickness of the water soluble component to the total aerosol optical thickness at λ=550nm ($\tau_{a,550}$). Optical thickness $\tau_{a,550}$ is then expressed. $\tau_{a,550}= f_w \tau_{a,550}+(1- f_w)\tau_{a,550} = \tau_{a,550}^{WS}+\tau_{a,550}^{OC}$, where $\tau_{a,550}^{WS}$ is the optical thickness of the water soluble component at λ=550nm, and $\tau_{a,550}^{OC}$, that of the oceanic component. For the other wavelengths, the optical thickness of aerosol is given by $\tau_{a,\lambda}= \tau_{a,\lambda}^{WS} + \tau_{a,\lambda}^{OC}$, where $\tau_{a,\lambda}^{WS} = \tau_{a,550}^{WS} \beta_{ext,\lambda}^{WS} / \beta_{ext,550}^{WS}$, and $\tau_{a,\lambda}^{OC} = \tau_{a,550}^{OC} \beta_{ext,\lambda}^{OC} / \beta_{ext,550}^{OC}$, where β_{ext} are the extinction coefficients. The Ångström exponent for the mixed aerosol model is obtained from $\tau_{a,\lambda}$. For the above model, the α value ranges from –0.10 for f_w=0 to 1.93 for f_w=1. The radiative transfer calculation was done for eight $\tau_{a,550}$ values (0.0, 0.02, 0.04, 0.08, 0.16, 0.32, 0.64, and 1.28) and six f_w values (0.0, 0.2, 0.4, 0.6, 0.8, and 1.0). The ocean surface is simulated by multiple facets whose slopes vary according to the wind speed over the ocean (Cox and Munk, 1954). The ocean wind speed is assumed to be 5m/sec. The effect of white caps is not taken into account. The ocean is assumed to be homogeneous with an optical thickness of 10. The ocean body is composed of pure water without hydrosols.

A look-up table of the radiation at the top of the atmosphere was created with five parameters: the solar zenith angle (θ_0), the satellite viewing angle (θ), the azimuth difference between solar and satellite viewing directions ($\phi-\phi_0$), the aerosol optical thickness at λ=550nm ($\tau_{a,550}$), and the Ångström exponent (α).

4.ALGORITHM

The principle of the algorithm can be seen in Figure 1. The relationships of the bi-directional reflectance (Fig. 1 (a)) and the degree of polarization (Fig. 1 (b)) between two wavelengths (670nm and 865nm) are shown as functions of the aerosol optical thickness at λ=550nm ($\tau_{a,550}$) and the Ångström exponent (α) in the normal plane ($\phi-\phi_0$=90°) for a moderate scattering angle (Θ=127°).

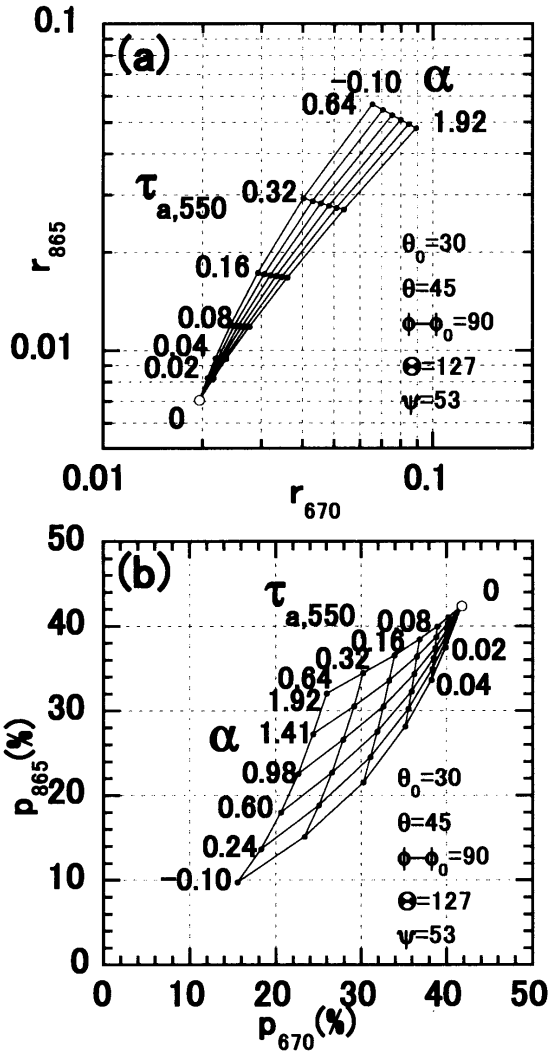

Figure 1 Relationship of (a) the bi-directional reflectance and (b) the degree of polarization between two wavelengths (670 and 865nm) as functions of the aerosol optical thickness at λ=550nm ($\tau_{a,550}$) and the Ångström exponent (α). The point for $\tau_{a,550}$=0 is shown by open circles. θ_0, solar zenith angle; θ, satellite viewing angle; ϕ-ϕ_0,azimuth difference angle; Θ, scattering angle; and Ψ, angle from the specular direction.

The bi-directional reflectance is defined as $\pi I/(F_0 \cos\theta_0)$, where I, F_0, and θ_0 are the intensity of radiation, the extraterrestrial incident solar flux density, and the solar zenith angle, respectively. Note that curves labeled by 1.92 (-0.10) correspond to the purely water soluble (oceanic) model. The $\tau_{a,550}$ and α values can be determined from the measurements of the radiance and/or the degree of polarization.

The outline of algorithm is as follows. First, the calculated radiance and degree of polarization is interpolated with respect to the cosine of the solar zenith angle, cosine of the satellite viewing angle, and azimuth difference. A two-dimensional table is then created for $\tau_{a,550}$=0.0 to 1.28 (steps=0.004 for $\tau_{a,550}$=0.0 to 0.04, 0.008 for $\tau_{a,550}$=0.04 to 0.08, 0.016 for $\tau_{a,550}$=0.08 to 0.16, 0.032 for $\tau_{a,550}$=0.16 to 0.32, 0.064 for $\tau_{a,550}$=0.32 to 0.64, and 0.128 for $\tau_{a,550}$=0.64 to 1.28), and for f_w=0.0 to 1.0 (step=0.05) by interpolating the calculations for eight $\tau_{a,550}$ values and six f_w values described in Section 3.

As mentioned previously, a target can be observed from up to 14 different viewing angles. The scattering angle (Θ) and the angle from the specular direction (ψ) change with the viewing direction. When the ψ value is small, the radiation at the top of the atmosphere may be contaminated by the radiation reflected by the ocean surface. The magnitude of influence is dependent on the surface wind velocity and direction. Even if the surface wind field were known, the relationship of the radiance between two wavelengths is not simple with respect to the change of $\tau_{a,550}$ and α (not shown). In the retrieval algorithm, the pixel with $\psi<\psi_{min}$ (=30°) is rejected. When the scattering angle (Θ) is large, the $\tau_{a,550}$ and α may be retrieved from the radiance. The viewing direction preferable for the polarization method is, however, limited by the scattering angle. The maximum scattering angle is about 135°, beyond which $\tau_{a,550}$ and α may not uniquely be determined (Masuda et al., 2000a). The most preferable image for a target is then selected based on the scattering angle ($\Theta_{min}<\Theta<\Theta_{max}$) and the effective area of 2-dimensional bi-directional reflectance and polarization diagrams (for example, Fig. 1 (a) and (b)).

Finally, the ($\tau_{a,550}$, α) pair which minimizes the following equation is selected.

$$d(\tau_{a,550}, \alpha)^2 = \Sigma_\lambda \{[(p_{c,\lambda}(\tau_{a,550}, \alpha) - p_{m,\lambda})/\sigma_{p\lambda}]^2 + [100*(r_{c,\lambda}(\tau_{a,550}, \alpha) - r_{m,\lambda})/ r_{m,\lambda}/ \sigma_{r\lambda}]^2\},$$

where the symbols p and r denote the degree of polarization (%) and bi-directional reflectance. Subscripts c and m refer to the calculation and measurement. λ refers to the wavelengths which are used for retrieval (670nm and 865nmm). $(1/\sigma)^2$ are weighting functions. It is reasonable to use some characteristic lengths (σ) in % for weighting functions. σ may be determined by considering measurement errors, possible retrieval errors caused by aerosol model assumption and so on. $(1/\sigma_{p\lambda}) = 0$ and $(1/\sigma_{r\lambda}) \neq 0$ corresponds to the radiance method; $(1/\sigma_{p\lambda}) \neq 0$, $(1/\sigma_{r\lambda}) = 0$, polarization method; $(1/\sigma_{p\lambda}) \neq 0$ and $(1/\sigma_{r\lambda}) \neq 0$, combined method.

5.RESULTS

Figure 2 shows (a) aerosol optical thickness at λ=550nm and (b) the Ångström exponent retrieved from the degree of polarization at wavelengths of 670 and 865nm by ADEOS/ POLDER near Japan on April 26, 1997 [$(1/\sigma_{p\lambda}) \neq 0$, $(1/\sigma_{r\lambda})$] = 0. Cloud indicator provided by CNES was used to distinguish cloud and clear areas. We classified a pixel as "clear" only if that pixel is indicated as "clear" from all viewing directions. Pixels with the scattering angle less than 135° is considered. Figures 3 (a) and (b) are the same as Figures 2 (a) and (b) except that they are retrieved from the bi-directional reflectance measurements [$(1/\sigma_{p\lambda}) = 0$ and $(1/\sigma_{r\lambda}) \neq 0$]

Figure 4 (a) shows frequency of occurrence (%) of $\tau_{a,550}$ differences between the polarization method and the radiance method for the same scattering angle (Θ<135°). Figure 4 (b) is the same as (a) but for the α. To create the histogram, we used the pixels which are located at least 2 pixels (about 25km) away from cloud or land areas.

From these figures, we can find that the $\tau_{a,550}$ retrieved from the bi-directional reflectance and the degree of polarization show similar values. On the other hand, the α values show some difference between the radiance and the polarization methods, where the α values retrieved from the degree of polarization are generally larger than those from the bi-directional reflectance.

Similar analysis was performed for the radiance method to examine the effect of scattering angle (Figure 5). The frequency of occurrence (%) of difference of $\tau_{a,550}$ and α retrieved using large scattering angles (150°<Θ<180°) and moderate scattering angles (75°<Θ<145°) is plotted. It is

(a) Optical thickness at 550nm ($\tau_{a,550}$)

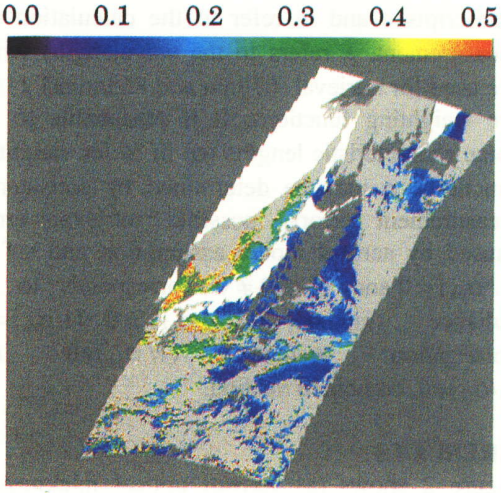

(b) Ångström exponent (α)

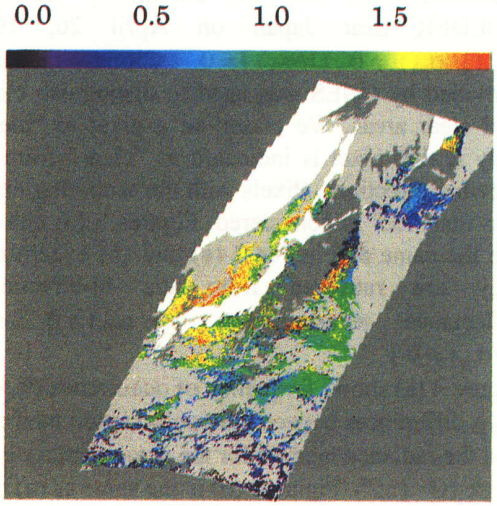

Figure 2 (a) Aerosol optical thickness at λ=550nm and (b) the Ångström exponent retrieved from the degree of polarization measurements at wavelengths of 670 and 865nm by ADEOS/ POLDER near Japan on April 26, 1997. Cloud: light gray, land: white, large scattering angle area: dark gray. Θ_{max}=135°. Results are displayed every two pixels in column and line directions; distance between pixels is about 13km.

(a) Optical thickness at 550nm ($\tau_{a,550}$)

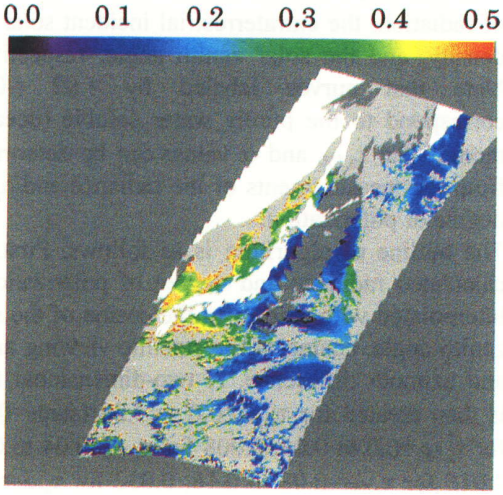

(b) Ångström exponent (α)

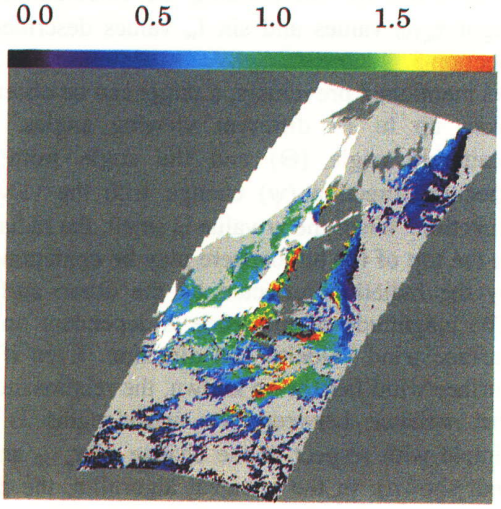

Figure 3 Same as Figure 2 but for retrieval from the bi-directional reflectance.

interesting that the $\tau_{a,550}$ values retrieved using large scattering angles are systematically smaller than those retrieved using moderate scattering angles for large optical thickness case ($\tau_{a,550}$>0.2). One of the reason may be non-sphericity effect of aerosol particles. It is well known that dust particles (yellow sand) originated from desert areas in China sometimes flow into east Asia around Japan in spring. The phase function of yellow dust particles is well simulated by semi-empirical phase functions of non-spherical particles (Nakajima et al., 1989), where the values of phase function at large scattering angles (150°<Θ) are much smaller (typically a factor of

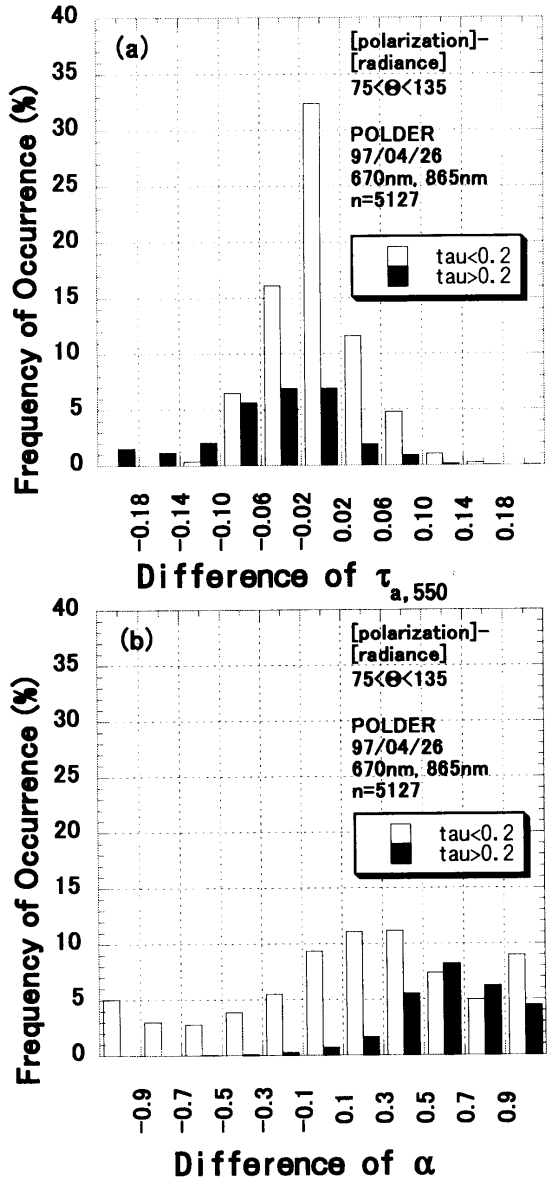

Figure 4 (a) Frequency of occurrence (%) of $\tau_{a,550}$ differences between the polarization method and the radiance method for the same scattering angle (Θ<135°). (b) Same as (b) but for α. open bars: $\tau_{a,550}$<0.2, solid bars: $\tau_{a,550}$>0.2.

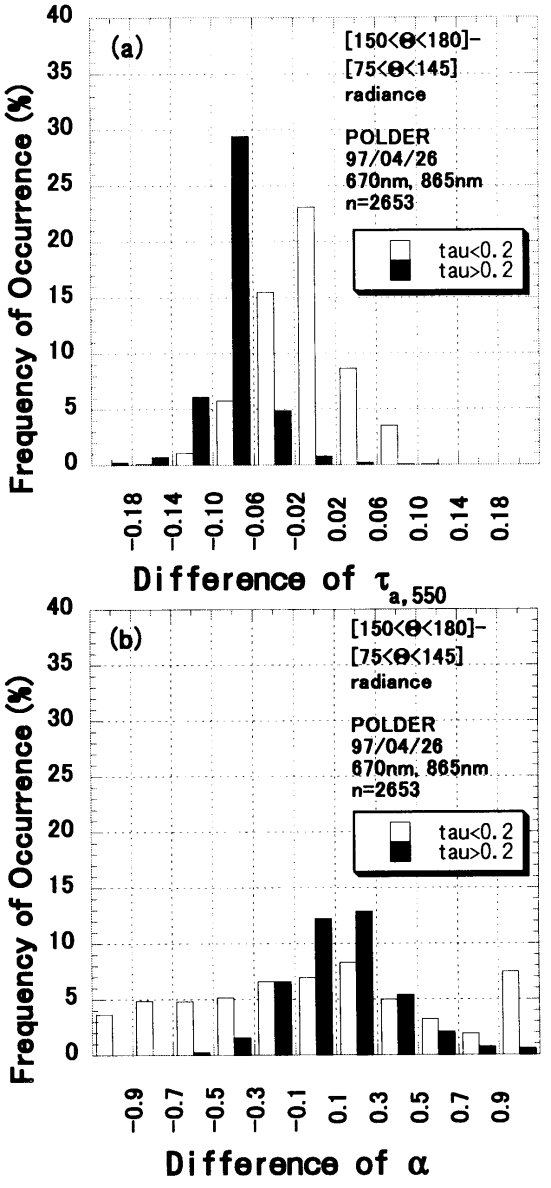

Figure 5 (a) Frequency of occurrence (%) of $\tau_{a,550}$ differences due to the scattering angle for the radiance method. (b) Same as (b) but for α. open bars: $\tau_{a,550}$<0.2, solid bars: $\tau_{a,550}$>0.2.

three) than those by spherical model. The shape of aerosol particles is assumed to be spherical in our model calculation. Consequently, retrieved optical thickness is underestimated for non-spherical particles. The opposite trend is seen at moderate scattering angle (Nakajima et al, 1989), which may result in overestimation of optical thickness for non-spherical particles. Therefore, the $\tau_{a,550}$ values retrieved at large scattering angles are smaller than those retrieved at moderate scattering angles.

6.SUMMARY

An algorithm is described to retrieve the optical thickness at a wavelength of 550nm and Ångström exponent of the aerosols over the ocean from the radiance and the degree of polarization

measurements by satellite. The algorithm is flexible in which the weights for the radiance and the degree of polarization are variable, by considering the effects of measurement and aerosol model assumption errors on retrieval.

The data acquired by ADEOS/POLDER on April 26, 1997 near Japan was investigated as a case study.

The optical thickness at 550nm showed similar values between the radiance and the polarization methods. This result suggests that the degree of polarization observed at moderate scattering angle (Θ<135°) may be used for long term monitoring of aerosol optical thickness over the ocean.

Retrievals of aerosol optical thickness using the radiance with different scattering angles showed a feasibility of detecting non-spherical particles.

Acknowledgments. POLDER data were provided by Centre National d'Etudes Spatiales, France. We sincerely thank Drs. T. Kobayashi, S. Mukai, I. Sano, Y. Kawata, and A. Yamazaki for their assistance of pre-processing of POLDER data and helpful discussions.

REFERENCES

Ångström, A., 1964, The parameters of atmospheric turbidity. *Tellus*, 16:64-75.

Cox, C and W. Munk, 1954, Statistics of the sea surface derived from sun glitter. *J.Mar. Res.*, 13:198-227.

Deschamps, P. Y., F. M. Bréon, M. Leroy, A. Podaire, A. Bricaud, J. C. Buriez, and G. Séze, 1994, The POLDER mission: instrument characteristics and scientific objectives. *IEEE Trans. Geosci. Remote Sen.*, 32:598-615.

Kneizys, F. X., and coauthors, 1980, *Atmospheric Transmittance/Radiance: Computer Code LOWTRAN5*. Air Force Geophysics Laboratory, AFGL-TR-80-0067, Hanscom AFB, MA.

Kneizys, F. X., and coauthors, 1988, *Users guide to LOWTRAN7*. Air Force Geophysics Laboratory, AFGL-TR-88-0177, Hanscom AFB, MA.

Masuda, K., H. Ishimoto, and T. Takashima, 2000a, Dependence of the spectral aerosol optical thickness retrieval from space on measurement error and model assumption. *Int. J. Remote Sens.*, submitted.

Masuda, K., M. Sasaki, T. Takashima, and H. Ishida, 1999, Use of polarimetric measurements of the sky over the ocean for spectral optical thickness retrievals. *J. Atmos. Oceanic Technol.*, 16:846-859.

Masuda, K., T. Takashima, Y. Kawata, A. Yamazaki, and M. Sasaki, 2000b, Retrieval of aerosol optical properties over the ocean using multispectral polarization measurements from space. *Applied Mathematics and Computation.*, 00:000-000, in press.

Nakajima, T, M. Tanaka, M. Yamano, M. Shiobara, K. Arao, and Y. Nakanishi, 1989, Aerosol optical characteristics in the yellow sand events observed in May, 1982 at Nagasaki – Part II Models, *J. Meteor. Soc. Japan*, 67:279-291.

World Climate Programme, WCP-55, 1983, *Report of the expert meeting on aerosols and their climate effects* (A. Deepak and H. E. Gerber, Eds.), World Meteorological Organization, Geneva.

World Climate Programme, WCP-112, 1986, *A preliminary cloudless standard atmosphere for radiation computation*, WMO/TD-No.24, World Meteorological Organization, Geneva.